Cellular/Molecular

Na^+ Channel-Dependent Recruitment of $Na_v\beta4$ to Axon Initial Segments and Nodes of Ranvier

Shelly A. Buffington and Matthew N. Rasband
Department of Neuroscience, Baylor College of Medicine, Houston, Texas 77030

The axon initial segment (AIS) and nodes of Ranvier are the sites of action potential initiation and regeneration in axons. Although the basic molecular architectures of AIS and nodes, characterized by dense clusters of Na^+ and K^+ channels, are similar, firing patterns vary among cell types. Neuronal firing patterns are established by the collective activity of voltage-gated ion channels and can be modulated through interaction with auxiliary subunits. Here, we report the neuronal expression pattern and subcellular localization of $Na_v\beta4$, the modulatory Na^+ channel subunit thought to underlie resurgent Na^+ current. Immunostaining of rat tissues revealed that $Na_v\beta4$ is strongly enriched at the AIS of a select set of neuron types, including many characterized by high-frequency firing, and at nodes of Ranvier in the PNS and some nodes in the CNS. By introducing full-length and mutant GFP-tagged $Na_v\beta4$ into cultured neurons, we determined that the AIS and nodal localization of $Na_v\beta4$ depends on its direct interaction with Na^+ channel α subunits through an extracellular disulfide bond. Based on these results, we propose that differences in the specific composition of the Na^+ channel complexes enriched at the AIS and nodes contribute to the diverse physiologies observed among cell types.

Introduction

High-density clusters of voltage-gated Na^+ channels decorate the axon initial segment (AIS) (Kole et al., 2008; Lorincz and Nusser, 2010). The activity of these AIS Na^+ channels regulates the probability of action potential (AP) initiation and contributes to overall neuronal excitability (Khaliq and Raman, 2006; Palmer and Stuart, 2006; Kole and Stuart, 2008). Na^+ channels undergo multiple posttranslational modifications, including glycosylation and phosphorylation, that influence their activation and inactivation kinetics. Na^+ channels are also influenced by interaction with auxiliary subunits (Isom et al., 1992). Na^+ channels comprise a pore-forming α subunit and modulatory β subunits. Four different $Na_v\beta$ subunits, termed $Na_v\beta1$–$Na_v\beta4$, are expressed in the nervous system. Of these, $Na_v\beta4$ is uniquely associated with resurgent Na^+ current (I_{NaR}), and its expression has been postulated to facilitate high-frequency AP generation during repetitive firing (Khaliq et al., 2003; Grieco et al., 2005).

Resurgent Na^+ current is a transient, voltage-dependent influx of Na^+ ions that occurs during repolarization of the membrane after strong depolarizations (Raman and Bean, 1997). Neurons expressing I_{NaR} are characterized by noncanonically short Na^+ channel refractory periods and heightened open-channel probability at subthreshold voltages. After depolarization, I_{NaR}-carrying channels are prevented from entering classical inactivation by the rapid insertion of an open-channel blocker (Raman and Bean, 2001). As repolarization proceeds, the pore blocker disengages from the α subunit allowing an influx of Na^+ ions as channels reopen before inactivating or reactivating. The C-terminal tail of $Na_v\beta4$ has been proposed as the open-channel blocker underlying resurgent kinetics (Grieco et al., 2005). Knockdown of $Na_v\beta4$ in cerebellar granule cells results in the loss of I_{NaR} and a decrease in repetitive firing (Bant and Raman, 2010). Inclusion of the putative blocking peptide in the recording pipette is sufficient to restore both properties in shRNA-treated cells, suggesting that $Na_v\beta4$ is indeed the endogenous open-channel blocker regulating I_{NaR}. Although $Na_v\beta4$ is most notably associated with I_{NaR}, its expression also increases persistent Na^+ current (I_{NaP}) (Aman et al., 2009), a current implicated in neocortical pyramidal neuron burst firing (Kole, 2011).

Despite recent studies implicating $Na_v\beta4$ as an important modulator of I_{NaR} and I_{NaP} (Grieco et al., 2005; Aman et al., 2009; Bant and Raman, 2010), the subcellular localization of $Na_v\beta4$ remains poorly characterized (Yu et al., 2003). Here, we report that $Na_v\beta4$ immunoreactivity is enriched at the AIS of cell types known to have I_{NaR}, including cerebellar Purkinje neurons and subthalamic neurons, among others (Bean 2007). We also observed layer-specific expression and AIS enrichment of $Na_v\beta4$ in cortical pyramidal neurons. Furthermore, we found $Na_v\beta4$ enriched at subsets of CNS and PNS nodes. Through mutational analysis, we identified the molecular mechanisms that regulate $Na_v\beta4$ recruitment to the AIS and nodes. These results provide molecular evidence that the expression pattern, subcellular localization, and molecular interactions of $Na_v\beta4$ are consistent with its proposed physiological role in regulating repetitive firing in multiple neuron types.

Received Aug. 23, 2012; revised Feb. 19, 2013; accepted Feb. 21, 2013.

Author contributions: S.A.B. and M.N.R. designed research; S.A.B. performed research; S.A.B. and M.N.R. analyzed data; S.A.B. and M.N.R. wrote the paper.

This work was supported by National Institutes of Health Grants NS073295 (S.A.B.) and NS044916 (M.N.R.). We thank Dr. James Trimmer and NeuroMab for generating the monoclonal α-$Na_v\beta4$ antibody and Dr. Yasuhiro Ogawa for generating the FL GFP-tagged $Na_v\beta4$ construct. We also thank Dr. Indira Raman and Dr. Maarten Kole for helpful discussions.

Correspondence should be addressed to Dr. Matthew N. Rasband, Department of Neuroscience, Baylor College of Medicine, One Baylor Plaza, BCM295, Houston, TX 77030. E-mail: rasband@bcm.edu.

DOI:10.1523/JNEUROSCI.4051-12.2013

 0270-6474/13/336191-12$15.00/0

Materials and Methods

Animals. Adult and timed-pregnant Sprague Dawley rats were purchased from Harlan Sprague Dawley. Animals were housed and maintained in Baylor College of Medicine's Center for Comparative Medicine, compliant with the National Institutes of Health *Guide for the Care and Use of Laboratory Animals*.

Antibodies. The following primary antibodies were used: mouse anti-α-$Na_v\beta4$ (N168/6 generated against a fusion protein including amino acids 184–228; NeuroMab), rabbit α-$Na_v\beta4$ F3888 (generated against a peptide, CKKLITFILKKTREK), rat α-GFP (04404-84; Nacalai Tesque), rabbit α-V5 (V8137; Sigma), mouse α-V5 (SV5-Pk1; AbD Serotec), rabbit α-$Na_v1.6$ (Rasband et al., 2003), rabbit α-βIV spectrin (Yang et al., 2004), mouse α-$K_v1.2$ (K14/16; NeuroMab), chicken α-MAP2 (EnCor Biotechnology), mouse α-ankyrin G (ankG) (N106/36; NeuroMab), mouse α-pan $Na_v\alpha$ (K58/35; Sigma), rabbit α-parvalbumin (PV) (NB120-11427; Novus Biologicals), rabbit α-calbindin (CB) (C2724; Sigma), mouse α-CB (AF2E5; Abcam), rabbit α-$K_v1.2$ (Rhodes et al., 1995), rat α-MBP (MAB386; Millipore), rabbit α-GFP (A11122; Invitrogen), mouse α-GFP (11E5; Invitrogen), mouse α-His tag (05-531; Millipore), rabbit α-GAPDH (G9545; Sigma), and mouse α-actin (MAB1501; Millipore). The following secondary antibodies were used: goat α-rat 488 (A11006; Invitrogen), goat α-mouse XA 594 (A11032; Invitrogen), goat α-mouse IgG1 488 (115-515-205; Jackson ImmunoResearch), goat α-mouse IgG2a 594 (115-515-206; Jackson ImmunoResearch), goat α-mouse IgG2b 594 (115-515-207; Jackson ImmunoResearch), goat α-rabbit 594 (A11037; Invitrogen), goat α-rabbit 488 (A11034; Invitrogen), goat α-mouse XA 350 (A21120; Invitrogen), goat α-chicken AMCA (103-155-155; Jackson ImmunoResearch), goat α-mouse HRP (A10551; Invitrogen), and goat α-rabbit HRP (G21234; Invitrogen) at 1:1000. Hoechst staining was used to identify nuclei in some experiments.

DNA and shRNA constructs. $Na_v\beta4$ was cloned from purified rat cDNA and inserted into vector pEGFP-N1. To generate the terminal truncation mutants, we subcloned the portion of interest out of the full-length (FL) $Na_v\beta4$ pEGFP–N1 construct and reinserted the product into empty pEGFP–N1 vector. Single point mutations were introduced into the FL, GFP-tagged $Na_v\beta4$ DNA by site-directed mutagenesis using the QuikChange Lightning kit (Agilent Technologies). Terminal truncations and single-point mutations of $Na_v\beta4$ DNA were verified by sequencing (GENEWIZ) and analysis using ApE (A Plasmid Editor) software. The efficacies of the Na^+ channel ($Na_v1.x$), neurofascin-186, and βIV spectrin shRNA expression plasmids were reported previously by Hedstrom et al. (2007).

Transfection and immunostaining of COS-1 cells. COS-1 cells were transfected with GFP-tagged $Na_v\beta4$, V5/His-tagged $Na_v\beta1$, or V5/His-tagged $Na_v\beta2$ mammalian expression vectors by lipid-based transfection. The $Na_v\beta1$ and $Na_v\beta2$ expression constructs were a gift from Dr. Doo Yeon Kim (Harvard Medical School, Boston, MA). COS-1 cells were seeded at 10% confluence and grown at 37°C in DMEM containing 10% fetal calf serum (FC-III), 1% Glutamax, and 1% penicillin–streptomycin (all from Invitrogen). Cells were transfected at ~60% confluency. Lipofectamine 2000 and cDNA were incubated separately in serum-free Opti-MEM and then combined and incubated 30 min at room temperature. The reaction mixture (2 μl Lipofectamine 2000/μg cDNA) was then added to the COS-1 cells, which were allowed to grow 48 h in the presence of the transfection reagents and then either fixed for immunostaining or scraped and suspended in reducing sample buffer for Western blotting.

Hippocampal neuron cultures. Hippocampal neurons were cultured essentially as in the study by Kaech and Banker (2006), in the absence of the glial feeder layer. In brief, hippocampi were isolated from the brains of E18 rat embryos, trypsin digested (0.25% trypsin in HBSS), and dissociated by trituration before plating on poly-L-lysine- and laminin-coated coverslips. Neuronal growth media (97% Neurobasal, 2% B-27 supplement, and 1% Glutamax; Invitrogen) was changed completely 4 h after plating and then supplemented, in part, with new media every 4 d.

Transfection of cultured hippocampal neurons. Hippocampal neurons were transfected either at the time of plating (DIV0) or on DIV11. For DIV0, immediately after dissection and dissociation, neurons were nucleofected with shRNA or cDNA expression plasmids using the Neon system (Invitrogen). The cells were dissociated, centrifuged, and resuspended in buffer T at a density of 24,000 cells/μl. A single 1400 mV pulse was delivered over 20 ms to electroporate the cell membrane and introduce cDNA and/or shRNA plasmids. Neurons were plated on poly-L-lysine- and laminin-coated coverslips at a final density of 250 cells/mm^2. Media was completely replaced 6 h after transfection. Hippocampal neurons were maintained from 1 to 3 weeks as indicated in primary neuron cultures methods section. For DIV11, Lipofectamine 2000 reagent (Invitrogen) was used to transfect DIV11 hippocampal neurons with $Na_v\beta4$ construct cDNA. Lipofectamine and cDNA were incubated separately in Neurobasal medium and then combined. After 30 min, the reaction containing 2 μl Lipofectamine 2000/μg DNA was added to the neurons. Media was completely replaced after 4 h incubation with the transfection reagent. Cells were allowed to mature 3 d and then fixed for additional processing on DIV14.

Myelinating cocultures. Myelinating cocultures were performed as described by Susuki et al. (2011). In brief, dorsal root ganglia (DRGs) were isolated from E16 rat embryos of either sex, dissociated, and plated on coverslips coated with Matrigel (BD Biosciences). Non-neuronal cells were eliminated by two rounds of incubation with anti-mitotic agents. The purified DRG were transfected with FL $Na_v\beta4$–GFP, $Na_v\beta4\Delta C$–GFP, $Na_v\beta4\Delta N$–GFP, or $Na_v\beta4$–C28A–GFP expression constructs on DIV9 using Lipofectamine LTX and PLUS reagents (Invitrogen). Purified rat Schwann cells (cultured as in the study by Susuki et al., 2011) were added at 10 DIV. Ascorbic acid was added at 15 DIV to induce myelination, and the cocultures were allowed to mature for 17 additional days. Cells were fixed in ice-cold, 4% paraformaldehyde for 20 min on DIV32 and then immunostained as described.

Western blots. Rat brains were rapidly extracted, and the regions were isolated in ice-cold cutting solution containing the following (in mM): 110 sucrose, 60 NaCl, 3 KCl, 1.25 NaH_2PO_4, 28 $NaHCO_3$, 0.5 $CaCl_2$, and 7 $MgCl_2$. The tissue was immediately snap frozen on dry ice. Frozen tissue was placed in ice-cold homogenization buffer containing the following: 40 mM HEPES, pH 7.5, 150 mM NaCl, 10 mM pyrophosphate, 10 mM glyceropyrophosphate, 1 mM EDTA, and 0.3% CHAPS, supplemented with protease inhibitor cocktail (Sigma) and the phosphatase inhibitors Na^+-fluoride (10 μM) and Na^+-orthovandate (10 μM). Membrane proteins were isolated by centrifugation. After protein quantification by BCA assay (Thermo Fisher Scientific), protein samples were diluted in either reducing or non-reducing SDS sample buffer (as indicated) and denatured at 95°C for 3 min. Subsequently, 10 or 50 μg protein/lane was loaded onto 7.5% SDS-PAGE gels, resolved, transferred onto nitrocellulose membranes, and probed overnight with the indicated primary antibodies in 5% milk, 0.2% Tween 20 TBS using standard techniques. HRP-conjugated secondary antibodies (1:1000) (Invitrogen) were used to visualize the primary antibodies. All Western blots were developed using enhanced chemiluminescence. Peroxidase activity was detected using the SuperSignal West Pico or Femto Chemiluminescence substrates (Thermo Fisher Scientific). Images were acquired on a luminescence image analyzer (GE Healthcare) through LAS4000 (GE Healthcare) software.

Immunostaining. For whole brain, optic nerve, spinal cord, and sciatic nerve, rats were killed by an overdose of isoflurane followed by exsanguination. Nervous system tissue was dissected rapidly. Brains were drop fixed in 4% PFA and 0.1 M PB for 1.5 h and equilibrated in 20% sucrose and 0.1 M PB over 48 h. Nerves were fixed in 4% PFA and 0.1 M PB for 30 min and equilibrated in 20% sucrose and 0.1 M PB for at least 24 h. Afterward, 30 μm brain/cerebellum or 12 μm longitudinal slices (optic nerve, sciatic nerve, and dorsal and ventral roots) were cut on a microtome and washed in 0.1 M PB. Slices were blocked in 10% normal goat serum and 0.1 M PB containing 0.3% Triton X-100 (PBTGS). Tissue was incubated overnight at 4°C in primary antibodies diluted in PBTGS. Primary antibodies were removed by washing the tissue three times for 5 min with PBTGS. Secondary antibodies were diluted in PBTGS and applied for 1 h at room temperature to visualize primary antibodies. Excess secondary antibodies were removed by consecutive 5 min washes with each of PBTGS, 0.1 M PB, and 0.05 M PB. Slices were mounted on 1% gelatin-coated coverslips. For cultured neurons, cells were fixed in ice-cold 4% PFA in 0.1 M PB at 4°C for 20 min. The PFA was removed by washing three times for 5 min with ice-cold 1× Dulbecco's phosphate

buffered saline. Cells were blocked and permeated in PBTGS for 30 min. Primary antibodies, diluted in PBTGS, were applied overnight at 4°C. The next day, primary antibodies were removed by washing three times for 5 min with PBTGS. Cells were stained with secondary antibodies for 1 h in the dark at room temperature and then washed one time for 5 min with each of PBTGS, 0.1 M PB, and 0.05 M PB. The coverslips were then air dried and mounted.

Imaging. Fluorescence imaging was performed on an AxioImager Z1 microscope (Carl Zeiss) fitted with an apotome and an AxioCam digital camera (Carl Zeiss). AxioVision acquisition software (Carl Zeiss) was used for collection of images. Images in the same dataset were acquired using uniform exposure times. Experiments were performed at least in triplicate. Fluorescence intensity was measured using NIH ImageJ. In some images, contrast and brightness were linearly adjusted using Photoshop (Adobe Systems). Image processing was applied uniformly across all images within a given dataset.

Statistical analyses and quantification. Two-tailed Student's *t* tests, with $p < 0.05$ as significance criteria, were used when appropriate. Results are displayed as mean ± SEM.

Results

Generation and validation of $Na_v\beta4$-specific antibodies

To determine the subcellular localization of $Na_v\beta4$, we generated rabbit polyclonal antibodies targeting epitopes within the C-terminal tail of $Na_v\beta4$ that include the putative open channel blocking peptide sequence (Grieco et al., 2005). In collaboration with the NIH-sponsored monoclonal antibody resource at University of California Davis, NeuroMab, we also generated mouse monoclonal antibodies targeting $Na_v\beta4$. We designed our antigenic peptides against the C terminus because it is unique among the Na^+ channel β subunits and does not share strong sequence identity with other proteins.

To test the specificity of the anti-$Na_v\beta4$ antibodies, we expressed GFP-tagged $Na_v\beta4$, V5/His-tagged $Na_v\beta1$, or V5/His-tagged $Na_v\beta2$ proteins in COS-1 cells. $Na_v\beta1$ and $Na_v\beta2$ share up to 35% sequence identity with $Na_v\beta4$. Immunostaining of Na^+ channel β subunit-transfected COS-1 cells confirmed the specificity of both the mouse monoclonal α-$Na_v\beta4$ (Fig. 1*A*) and rabbit polyclonal α-$Na_v\beta4$ antibodies for $Na_v\beta4$ (Fig. 1*B*). $Na_v\beta4$ immunoreactivity colocalized with GFP in the $Na_v\beta4$-transfected cultures but was undetectable in the $Na_v\beta1$–V5/His- and $Na_v\beta2$–V5/His-transfected cells that showed positive immunoreactivity when immunostained for V5 (Fig. 1*A*,*B*) or His (data not shown) tags. Immunoblotting of protein homogenates collected from COS-1 cells transfected with one of the three tagged $Na_v\beta$ subunit constructs (Fig. 1*C*) showed a single band at ~63 kDa in the $Na_v\beta4$–GFP-transfected cell homogenates when immunolabeled with the α-$Na_v\beta4$ antibodies (Fig. 1*C*, mouse monoclonal, *D*, rabbit polyclonal) or an antibody against GFP. To test the specificity of the α-$Na_v\beta4$ antibodies on neuronal cells, we performed immunoblots on rat whole-brain membrane protein homogenates. By immunoblot, the mouse monoclonal $Na_v\beta4$ antibody recognized a single band at 38 kDa (Fig. 1*D*), a molecular mass consistent with previous reports of $Na_v\beta4$ (Yu et al., 2003). Similarly, the rabbit polyclonal $Na_v\beta4$ antibody recognized the 38 kDa $Na_v\beta4$ band. However, this antibody also recognized a nonspecific band around 110 kDa (Fig. 1*D*, denoted by *). Together, these results demonstrate that the antibodies used in this study recognize $Na_v\beta4$ and do not cross-react with the Na^+ channel β subunits $Na_v\beta1$ or $Na_v\beta2$.

$Na_v\beta4$ is enriched at AIS of diverse cell types

To determine the general expression pattern of $Na_v\beta4$, we performed Western blots on rat membrane protein homogenates isolated from discrete brain regions. Immunoblotting for $Na_v\beta4$ revealed single immunoreactive bands at ~38 kDa in each tissue examined, excluding the optic nerve (Fig. 2*A*). The lack of $Na_v\beta4$ detected in the optic nerve likely reflects the low amount of $Na_v\beta4$ protein relative to the total protein in the homogenate (see also Fig. 4). The wide distribution of $Na_v\beta4$ protein expression is

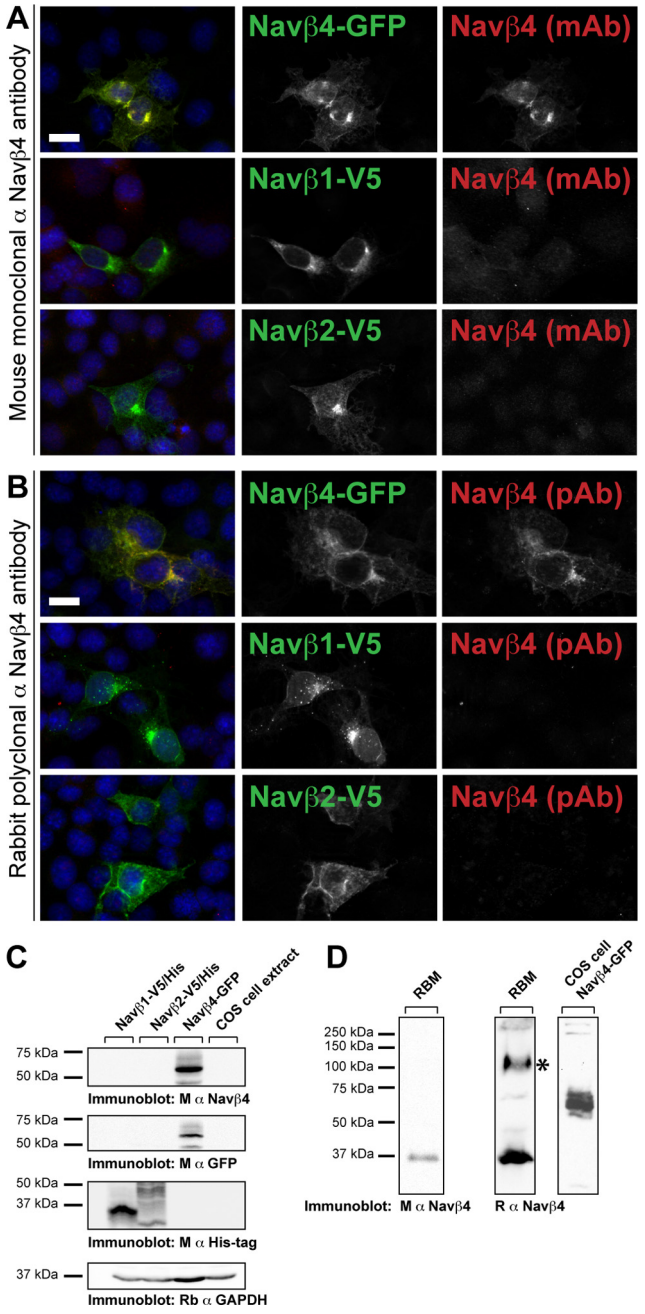

Figure 1. α-$Na_v\beta4$ antibodies do not cross-react with $Na_v\beta1$, $Na_v\beta2$, or other AIS proteins. ***A***, ***B***, COS cells expressing $Na_v\beta4$–GFP, $Na_v\beta1$–His/V5, or $Na_v\beta2$–His/V5 immunostained for either GFP or V5 (green), as appropriate, and $Na_v\beta4$ (red). ***A***, Mouse monoclonal α-$Na_v\beta4$. ***B***, Rabbit polyclonal α-$Na_v\beta4$. Nuclei were labeled with Hoechst stain (blue in the merged image). Scale bars, 20 μm. ***C***, Western blotting of COS cell protein lysates immunoblotted using α-$Na_v\beta4$ antibodies and antibodies to detect either the GFP- or His-tagged $Na_v\beta$ subunits. ***D***, Immunoblots of rat brain membrane (RBM) protein homogenates or $Na_v\beta4$–GFP-transfected COS cells, as indicated, probed for $Na_v\beta4$, which has an approximate molecular weight of 38 kDa. A nonspecific band in the rat brain membrane homogenate recognized by the rabbit polyclonal antibody against $Na_v\beta4$ is denoted with an asterisk. M, Mouse; R, rat.

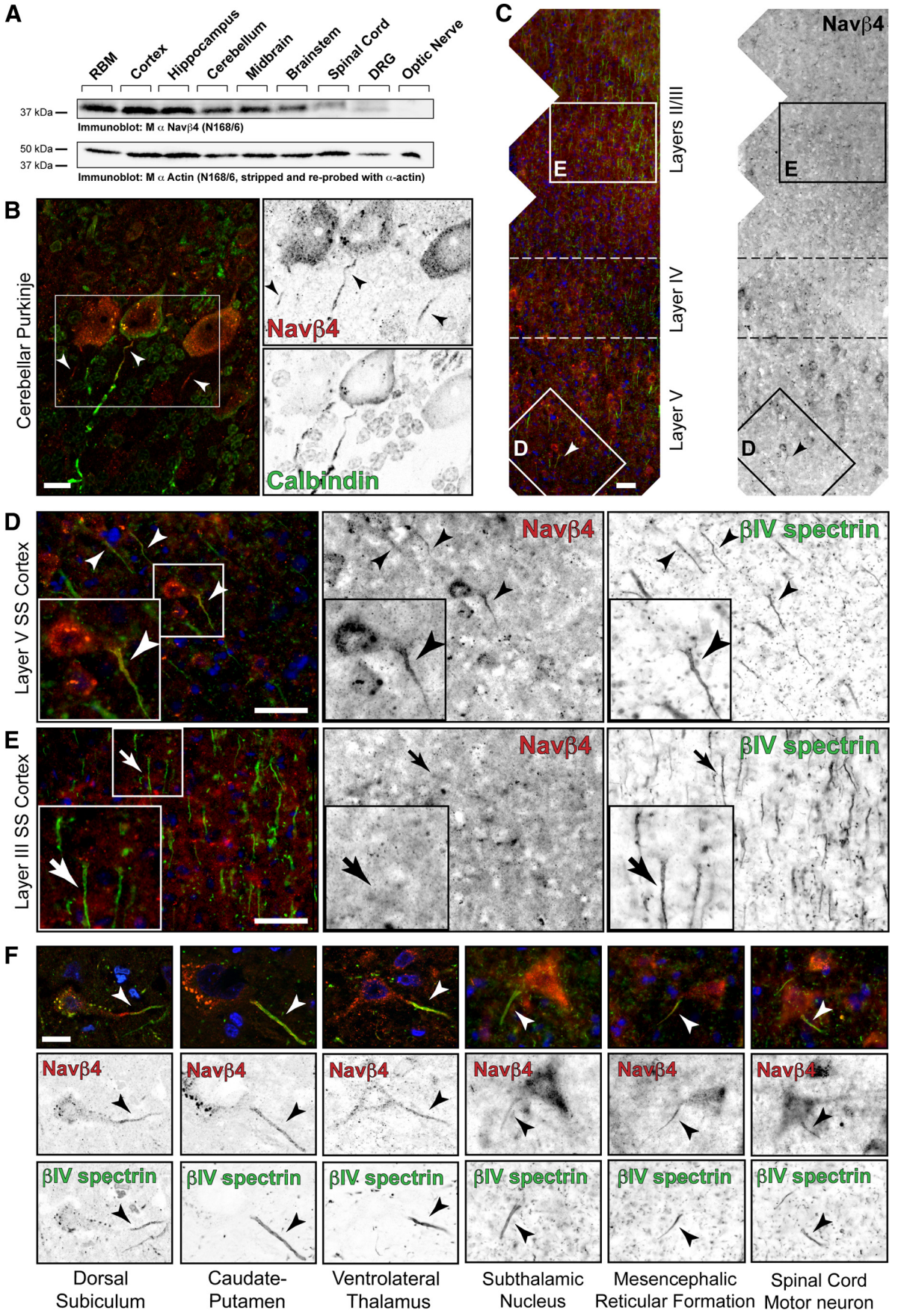

Figure 2. Immunolocalization of $Na_v\beta4$ reveals AIS enrichment in multiple CNS cell types. ***A***, Western blot of brain-region-specific homogenates probed with the mouse (M) monoclonal α-$Na_v\beta4$ antibody. Immunoblotting for actin served as a loading control. RBM, Rat brain membrane. ***B–F***, Immunostaining of multiple brain regions for $Na_v\beta4$ (mouse (*Figure legend continues.*)

Table 1. $Na_v\beta4$ expression in PV/CB-expressing cells

	Express Nav$\beta4$ (%)	AIS Nav$\beta4^+$ (%)
Layer V cortex		
PV^+/CB^+	100.0 ± 0	42.9 ± 14.3
PV^-/CB^+	41.5 ± 1.5	16.1 ± 4.8
PV^+/CB^-	81.6 ± 9.2	26.2 ± 4.1
Layer II/III cortex		
PV^+/CB^+	100.0 ± 0	100.0 ± 0
PV^-/CB^+	21.7 ± 2.1	0.9 ± 1.08
PV^+/CB^-	40.7 ± 13.0	10 ± 2.7
Hippocampus		
PV^+/CB^+	87.1 ± 1.9	73.1 ± 2.3
PV^-/CB^+	96.0 ± 1.5	67.5 ± 1.5
PV^+/CB^-	78.2 ± 2.9	40.7 ± 13.0
Trapezoid body		
PV^+/CB^+	99.0 ± 1.0	66.0 ± 0.4
PV^-/CB^+	96.7 ± 3.3	63.0 ± 6.2
PV^+/CB^-	100 ± 0.0	100 ± 0.0
Purkinje neurons		
PV^+/CB^+	100.0 ± 0	88.3 ± 1.3

Quantification of the percentage of total interneurons expressing $Na_v\beta4$ and the percentage of cells with detectable $Na_v\beta4$ enrichment at the AIS in layer V ($N = 3$, $n = 54$) and layer II/III cortex ($N = 3$, $n = 52$) and in the hippocampus ($N = 3$, $n = 52$). Quantification of $Na_v\beta4$ expression and AIS localization in PV/CB-expressing cells of the TB ($N = 3$, $n = 52$) and cerebellar Purkinje neurons ($N = 3$, $n = 100$) is also reported. Cells were triple labeled with antibodies detecting $Na_v\beta4$ (mouse monoclonal), CB, and PV. $Na_v\beta4$-expressing cells that were CB^- and PV^- were excluded from the analysis. Data are presented as the average ± SEM value.

consistent with previously published reports of $Na_v\beta4$ expression by RT-PCR and *in situ* hybridization (Yu et al., 2003).

Resurgent Na^+ current has been observed in only a subset of neuron types, and $Na_v\beta4$ has been proposed to underlie both I_{NaR} and I_{NaP} (Grieco et al., 2005; Aman et al., 2009). Therefore, we considered whether (1) $Na_v\beta4$ expression correlates with I_{NaR}, (2) $Na_v\beta4$ expression is most pronounced in cells that fire rapidly, and (3) $Na_v\beta4$ colocalizes with the dense clusters of sodium channels enriched at sites of AP generation (the AIS) and propagation (nodes of Ranvier). Immunostaining of brain sections revealed markedly heterogeneous cell-type-specific expression of $Na_v\beta4$ protein at the AIS of many different cell types (Fig. 2*B–F*). In cerebellar sections, $Na_v\beta4$ immunoreactivity was evident in 100% of Purkinje neuron somata; of these, 88.3 ± 1.3% ($N = 3$, $n = 100$) had enriched $Na_v\beta4$ immunoreactivity at the AIS (Fig. 2*B*; Table 1). Interestingly, in the neocortex, $Na_v\beta4$ was most strongly expressed in layer V pyramidal neurons and neighboring, PV-positive (PV^+) interneurons (Figs. 2*C–E*, 3*A*, Table 1). Colabeling for the AIS protein βIV spectrin showed that $Na_v\beta4$ is highly enriched at the AIS of layer V pyramidal neurons (Fig. 2*D*) but is essentially undetectable at layer II/III neuron AIS (Fig. 2*E*) (74.0 ± 4.4 vs 5.0 ± 4.4% βIV spectrin$^+$ AIS were $Na_v\beta4^+$, respectively; $N = 3$, $n = 200$), suggesting layer-specific mechanisms of Na^+ channel modulation. $Na_v\beta4$ immunoreactivity was also enriched at the AIS of a subset of neurons in the dorsal subiculum, the striatum, the ventrolateral thalamus, the subthalamic nucleus, the mesencephalic reticular formation, and spinal cord motor neurons (Fig. 2*F*). Thus, although $Na_v\beta4$ expression is not a fail-safe predictor of I_{NaR} (cultured spinal neurons have been reported to express only small, if any, resurgent currents; Pan and Beam, 1999), we identified $Na_v\beta4$ protein expression in several cell types reported previously to express I_{NaR} (Bean, 2007). Notably, $Na_v\beta4$ immunoreactivity was not detected in hippocampal area CA1 or CA3 pyramidal neuron AIS, which is consistent with the low levels of mRNA expression and the rare observation of I_{NaR} in these neuron types (Yu et al., 2003; Castelli et al., 2007a). Together, these results suggest that there is diversity in the molecular composition of the AIS across cell types. To the best of our knowledge, $Na_v\beta4$ is one of the first modulatory ion channel subunits to be identified as a cell-type-specific AIS protein.

Currently, it remains unknown whether fast-spiking interneurons express $Na_v\beta4$ protein. Several classes of physiologically distinct interneurons exist throughout the brain. Beyond their anatomical location, these can be further distinguished by their molecular expression profiles and their innervation patterns onto target cell subcellular domains (Klausberger and Somogyi, 2008; Klausberger, 2009). To begin to determine which, if any, interneuron types express $Na_v\beta4$, we colabeled tissue sections with α-$Na_v\beta4$ antibodies and antibodies targeting the interneuron-specific calcium-binding proteins PV and CB. Triple immunostaining showed $Na_v\beta4$ in a reticular pattern surrounding the nucleus as well as AIS-specific enrichment in a subset of cells characterized by PV and/or CB expression (Fig. 3; Table 1). $Na_v\beta4$ immunoreactivity was evident in 81.6 ± 9.2% of the PV-expressing interneurons in layer V neocortex and at 78.2 ± 2.9 in the hippocampal CA1 region and the subiculum (Figs. 3*A*,*B*; Table 1). Layer V PV/CB^+ cells uniformly expressed $Na_v\beta4$ in layer V cortex, but $Na_v\beta4$ was only enriched at the AIS of 42.9 ± 14.3% of these (Fig. 3*A*). In layer II/III cortex, $Na_v\beta4$ was expressed in 40.7% of PV-expressing interneurons but was evident at the AIS of only 6.7 ± 6.7% of these cells [$N = 3$, $n = 52$ (N is the number of animals, and n is the number of cells analyzed per animal)] (Fig. 3*A*). Although PV/CB^+ basket cells were infrequently encountered in layer II/III cortex, all of those identified had $Na_v\beta4^+$ AIS. However, PV^+ interneurons in the cortex/amygdala transition did not show $Na_v\beta4$ immunoreactivity ($N = 3$, $n = 10$). Among the CB-expressing, PV-negative (PV^-) interneurons quantified, those in the hippocampus were the most likely to express $Na_v\beta4$, with 96.0 ± 1.5% of the population expressing $Na_v\beta4$, and 70.3 ± 1.9% of those had detectable $Na_v\beta4$ immunoreactivity at the AIS ($N = 3$, $n = 52$) (Fig. 3*B*; Table 1). CB^+ neurons of the inferior colliculus and other brainstem regions had strong somatic and AIS-enriched $Na_v\beta4$ immunoreactivity, consistent with the findings of Kodama et al. (2012). Our data suggest that a subset of fast-spiking interneurons, including PV/CB^+ interneurons of the cortex and hippocampus, express $Na_v\beta4$ and that many of these have AIS enrichment of $Na_v\beta4$; however, we also observed $Na_v\beta4$ expression in CB-expressing, PV^- cells that have been reported to fire at uniformly low rates (Hartwich et al., 2009). Quantification of $Na_v\beta4$ expression in interneuron populations of discrete brain regions is provided in Table 1.

During these studies, we also noted strong expression of $Na_v\beta4$ in the somata and at the AIS of the PV/CB-expressing neurons of the trapezoid body (TB) [99.0 ± 1.0% PV^+/CB^+ TB neurons were $Na_v\beta4^+$, whereas $Na_v\beta4$ was specifically enriched at the AIS of 66.7 ± 0.6% of these ($N = 3$, $n = 52$)] (Fig. 3*C*,*D*). Therefore, $Na_v\beta4$ may contribute to the resurgent sodium currents displayed by principle neurons in the medial nucleus of the TB, which are thought to be modulated by factors other than α

←

(*Figure legend continued.*) monoclonal; red) and CB (***B***, green) or βIV spectrin (***C–F***, green). Hoechst nuclear staining is shown in blue in the merged images. ***B***, Immunostaining of cerebellar sections for $Na_v\beta4$ (red) and the Purkinje cell marker CB (green). ***C***, Immunostaining of somatosensory cortex showing layer-specific enrichment of $Na_v\beta4$ expression. Boxes ***D*** and ***E*** are expanded in the subsequent panels. ***F***, Representative images of $Na_v\beta4$-expressing neurons in the indicated brain regions. AIS enrichment is demonstrated by colocalization with βIV spectrin. Scale bars: ***B***, ***F***, 20 μm; ***C–E***, 40 μm.

subunits (Leão et al., 2006). Together, these data highlight the heterogeneity of $Na_v\beta4$ expression among cell types.

$Na_v\beta4$ is enriched at nodes of Ranvier

In myelinated axons, APs are regenerated at nodes of Ranvier. Nodes and the AIS share a common molecular composition, including dense clusters of voltage-gated Na^+ channels that underlie the depolarizing phase of the AP. Furthermore, because some peripheral sensory neurons can support trains of APs at frequencies approaching 1 kHz (Wellnitz et al., 2010), we wondered whether $Na_v\beta4$ also modulates Na^+ channels enriched at nodes. To test this idea, we immunostained CNS and PNS nerves with antibodies against $Na_v\beta4$, the nodal marker βIV spectrin, and juxtaparanodal $K_v1.2$ channels (Fig. 4*A*). We found that $Na_v\beta4$ immunoreactivity colocalized with βIV spectrin at a subset of optic nerve (31.3 ± 2.7%), ventral root (88.3 ± 1.9%), and dorsal root (72.3 ± 3.8%) nodes of Ranvier (Fig. 4*B*). On closer examination, we determined that there is a small but statistically significant increase in the probability of $Na_v\beta4^+$ immunoreactivity at nodes of large- versus small-diameter axons (82.0 ± 1.0 vs 67.5 ± 4.2% $Na_v\beta4^+$, respectively; $p = 0.015$) (Fig. 4*C*,*D*). Axons ≥4 μm in diameter were counted among the large axons, whereas those ≤3 μm in diameter were classified as small. No significant difference was found between the probabilities of $Na_v\beta4$ enrichment at large versus small ventral root axons (90.7 ± 1.5 vs 92.3 ± 2.3%, respectively; $p = 0.58$) (Fig. 4*C*,*D*). These results demonstrate that $Na_v\beta4$ is enriched at a subset of nodes of Ranvier in both the CNS and PNS and suggest that $Na_v\beta4$ modulation of nodal Na^+ channels may contribute to either I_{NaP} or I_{NaR} at nodes of Ranvier during AP propagation.

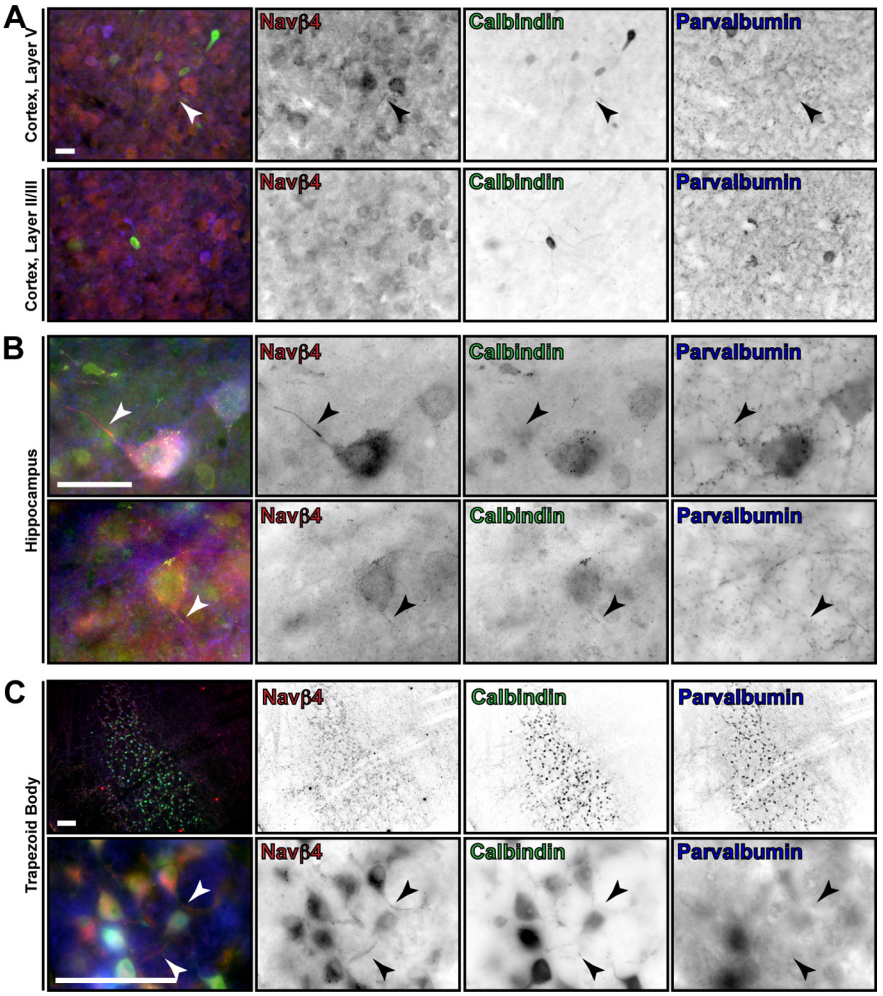

Figure 3. $Na_v\beta4$ is enriched at interneuron AIS. ***A–C***, Triple immunostaining of $Na_v\beta4$ (red) (mouse monoclonal antibody) with the calcium binding proteins CB and PV in green or blue, as indicated. Arrowheads highlight $Na_v\beta4^+$ AIS. Scale bars: ***A***, ***B***, 40 μm; ***C***, 80 μm. ***A***, Immunostaining of somatosensory cortex layers V and II/III, as indicated. The $Na_v\beta4^+$ layer V pyramidal neuron AIS is highlighted by the arrow in the top row. The bottom row displays the relatively low expression of $Na_v\beta4$ among both the excitatory pyramidal neurons and CB and/or PV^+ interneurons of layer II/III cortex. ***B***, Immunostaining of $Na_v\beta4^+$ interneurons in the hippocampus. Arrowhead points to the $Na_v\beta4^+$ AIS of the CB/PV^+ hippocampal interneuron featured in the top row. The arrowhead in the bottom row highlights the $Na_v\beta4^+$ AIS of the CB-expressing, PV^- hippocampal neuron featured in the bottom row. ***C***, Immunostaining of the TB showing $Na_v\beta4$ expression and AIS-enrichment in the CB/PV-expressing cells, indicated by the arrowheads. Scale bars, 80 μm.

AIS localization of $Na_v\beta4$ requires ankG and Na^+ channel α subunit expression

Na^+ channel α subunit recruitment to AIS and nodes of Ranvier is mediated through an ankyrin-binding motif located within the II–III cytoplasmic linker of the channels (Garrido et al., 2003; Lemaillet et al., 2003; Gasser et al., 2012). Similarly, neurofascin-186 and βIV spectrin localization to the AIS also require binding to ankG (Zhang et al., 1998; Yang et al., 2007). To determine how $Na_v\beta4$ is recruited to the AIS, we first determined whether FL GFP-tagged $Na_v\beta4$ constructs localize to the AIS in cultured hippocampal neurons. Cells were transfected at the time of plating and allowed to mature DIV14 before analysis. Immunostaining of transfected neurons revealed AIS-specific enrichment of $Na_v\beta4$–GFP protein (Fig. 5*A*). In contrast, and consistent with our immunofluorescence results from brain sections, we did not detect any endogenous $Na_v\beta4$ expression in cultured hippocampal pyramidal neurons (Fig. 5*B*). Thus, exogenously introduced GFP-tagged $Na_v\beta4$ protein can localize to the AIS without additional factors unique to I_{NaR}-expressing cells.

To determine whether the subcellular distribution of $Na_v\beta4$ depends on ankG, we cotransfected cells with FL GFP–$Na_v\beta4$ and either ankG-targeted or control shRNA constructs. Knockdown of ankG disrupted $Na_v\beta4$ targeting to the AIS in 100% of transfected neurons ($N = 3$, $n = 100$; Fig. 5*C*). To test whether the ankG-dependent recruitment of Na^+ channel α subunits is required for $Na_v\beta4$ enrichment at the AIS, we cotransfected GFP-tagged $Na_v\beta4$ with Na_v1-targeted shRNA. $Na_v\beta4$ AIS localization was completely abolished in the absence of Na_v1 α subunit expression, indicating that this interaction is required for $Na_v\beta4$ recruitment to the AIS (Fig. 5*C*). Thus, although ankG expression is necessary for AIS localization of $Na_v\beta4$, it is not sufficient for it but instead requires coexpression and AIS localization of Na^+ channel α subunits. However, knockdown of other AIS proteins, including βIV

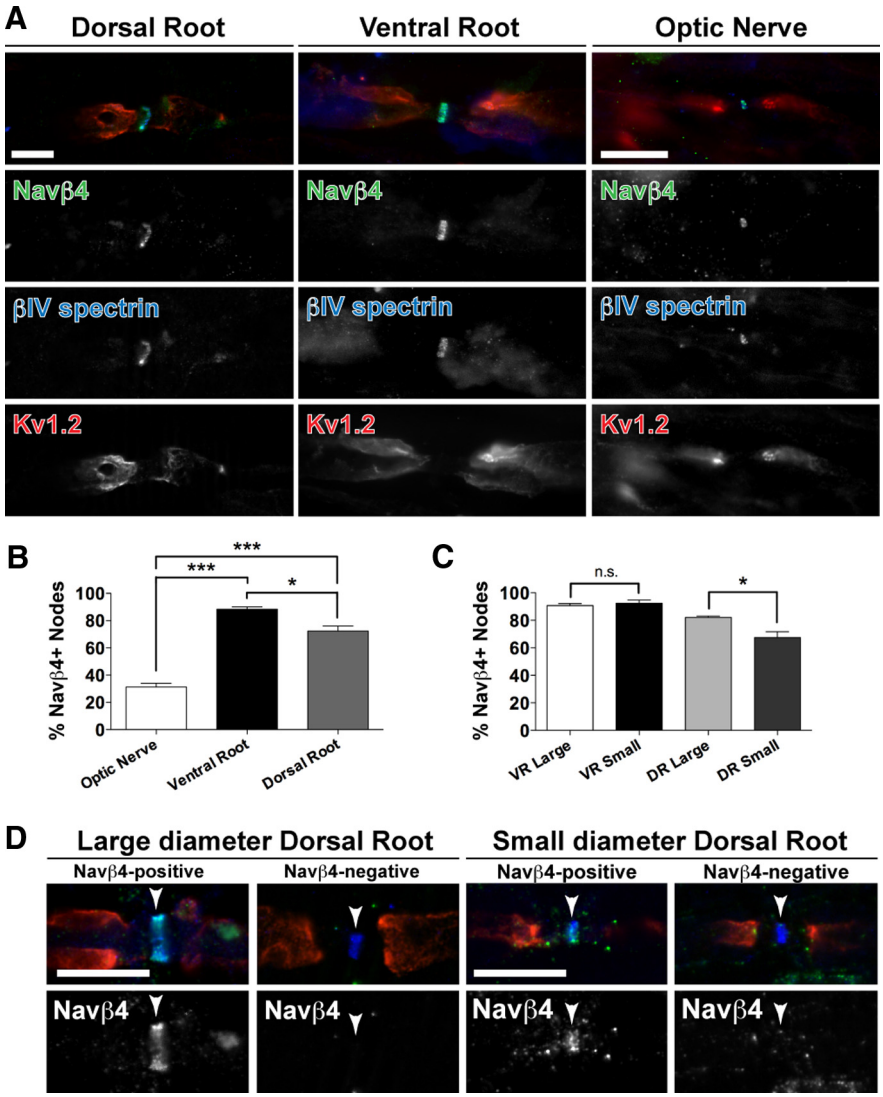

Figure 4. $Na_v\beta4$ is enriched at a subset of CNS and PNS nodes of Ranvier. ***A***, Immunostaining of rat dorsal and ventral spinal cord roots and optic nerve using antibodies against $Na_v\beta4$ (rabbit polyclonal; green), nodal βIV spectrin (blue), and juxtaparanodal $K_v1.2$ channels (red). ***B***, Quantification of the percentage of nodes with detectable $Na_v\beta4$ immunoreactivity enrichment in the indicated nerve types ($n = 100$, $N = 3$). ***C***, Quantification of $Na_v\beta4^+$ nodes in large- vs small-diameter ventral (VR) and dorsal (DR) root axons ($n = 100$, $N = 4$). $^*p < 0.05$, $^{***}p < 0.001$. Error bars represent SEM. ***D***, Images show representative examples of $Na_v\beta4^+$ and $Na_v\beta4^-$ large- and small-diameter dorsal root nodes coimmunostained for βIV spectrin (blue) and $K_v1.2$ (red), shown in the merged images. Scale bars, 10 μm.

spectrin and neurofascin-186, had no effect on the subcellular distribution of $Na_v\beta4$ (Fig. 5*D*). These data show that $Na_v\beta4$ enrichment at the AIS requires Na^+ channel α subunits.

Cysteine 28 is essential for $Na_v\beta4$ recruitment to the AIS

Similar to $Na_v\beta1$ and $Na_v\beta2$, $Na_v\beta4$ comprises an extracellular Ig-like fold, a single transmembrane domain, and a short C-terminal tail. The N-terminal Ig-like fold of β4 is structurally similar to those of β1 and β2. The extracellular domains of the β subunits are thought to be critical to their function; indeed, β1 has been proposed to function not only in Na^+ channel modulation but also in cell adhesion with a role in neurite outgrowth during postnatal CNS development (Brackenbury et al., 2008). The C-terminal tail of $Na_v\beta4$ is unique among the $Na_v\beta$ subunits and contains the putative open channel blocking peptide.

To determine how $Na_v\beta4$ interacts with Na^+ channel α subunits, we expressed FL and mutant GFP-tagged $Na_v\beta4$ constructs in cultured hippocampal neurons. First, we transfected terminal truncation mutants in which either the C or N terminus of $Na_v\beta4$ was deleted. Like FL $Na_v\beta4$–GFP, we found $Na_v\beta4\Delta C$–GFP enriched at the AIS of 100% of transfected neurons (Fig. 6*A*). In contrast, the N-terminal deletion completely abolished the AIS localization of $Na_v\beta4$ (Fig. 6*A*). Therefore, the determinants of AIS targeting in $Na_v\beta4$ are contained within its extracellular N-terminal domain.

The N terminus of $Na_v\beta4$ has three cysteine residues. By analogy to β1 and β2, two of these, C23 and C101, are thought to provide an internal disulfide bond to stabilize the quaternary structure of the extracellular domain (Barbieri et al., 2012). However, the third cysteine, C28, is left unpaired with the potential to form an extra-molecular covalent disulfide bond (Yu et al., 2003). Single point mutation of C28 to alanine ($Na_v\beta4$–C28A) resulted in disrupted $Na_v\beta4$ targeting, similar to the ΔN results (Fig. 6*B*,*D*). For additional analysis, we generated single point mutations of C23 and C101 as well as amino acids that were either within close proximity or well separated from the cysteines. Mutation of either paired cysteine, C23 or C101, also disrupted AIS localization of $Na_v\beta4$ (Fig. 6*C*,*D*), presumably as a result of disruption of the Ig-like fold causing C28 to no longer be positioned for favorable interaction with the reciprocal α subunit cysteine. Single point mutation of G30 and L21 to alanine also caused mislocalization of $Na_v\beta4$, whereas mutation of $Na_v\beta4$ at G52 (Fig. 6*C*), T24, T45, V63, and V103 preserved AIS localization (Fig. 6*D*).

In support of the idea that $Na_v\beta4$ and Na_v1 α subunits form a covalent disulfide linkage, we found that a single 38 kDa immunoreactive band was present in Western blots of brain membrane homogenates denatured in reducing sample buffer and probed for $Na_v\beta4$. In contrast, when the proteins were denatured in non-reducing sample buffer, two bands were evident after probing for $Na_v\beta4$: the first at 38 kDa, representing $Na_v\beta4$ alone, and the second at a molecular weight (>250 kDa) corresponding to $Na_v\beta4$ linked to an α subunit (Fig. 6*E*). These findings are consistent with previous reports (Yu et al., 2003). Together, the data presented in Figures 5 and 6 demonstrate that $Na_v\beta4$ recruitment to the AIS depends on its direct interaction with Na_v1 α subunits through a disulfide bond mediated by C28 in $Na_v\beta4$.

$Na_v\beta4$ localization at nodes of Ranvier requires disulfide linkage to α subunits

Although they share a common molecular organization, recent studies show that the mechanisms governing AIS assembly differ from those at nodes (Hedstrom et al., 2008; Feinberg et al., 2010; Zhang et al., 2012). ankG localization in the proximal axon is

essential for AIS formation because all other AIS proteins, including Na^+ channels, are recruited to the AIS through either direct or indirect linkage to ankG (Hedstrom et al., 2008). Whereas ankG clustering at the AIS is specified completely by the neurons, Na^+ channel clustering at nodes of myelinated axons depends on neuron–glia interactions (Eshed et al., 2005; Feinberg et al., 2010; Galiano et al., 2012; Zhang et al., 2012). It is possible that Na$_v\beta$4 localization to nodes occurs independently of Na^+ channel localization, because previous reports suggest that Na$_v\beta$1 directly interacts with other axonal and glial cell adhesion molecules, including neurofascin-186 and NrCAM (McEwen and Isom, 2004). To determine whether a disulfide-mediated interaction between Na$_v\beta$4 and Na^+ channel α subunits is necessary for Na$_v\beta$4 clustering along myelinated axons, we used an *in vitro* DRG neuron–Schwann cell myelinating coculture system. Purified DRG neurons were prepared from embryonic rat pups in parallel with purified Schwann cells from P2 rats. DRG neurons were transfected with either the FL, ΔC, ΔN, or C28A GFP-tagged Na$_v\beta$4 expression constructs on DIV10 and then combined with Schwann cells at DIV11. Myelination was induced 1 week later. After 2 weeks of myelination, we fixed the neurons and immunostained for GFP, the myelin marker MBP, and nodal marker ankG. Similar to our AIS results, we found that the FL and ΔC Na$_v\beta$4–GFP proteins colocalized with ankG at heminodes (heminodes are precursors to nodes of Ranvier) (heminodes FL Na$_v\beta4^+ = 94.5 \pm 3.9\%$, $n = 66$, $N = 3$; heminodes Na$_v\beta4\Delta C^+ = 94.6 \pm 2.6\%$, $n = 76$, $N = 3$) (Fig. 7*A*,*C*). In contrast, we found that the ΔN- and C28A–Na$_v\beta$4–GFP proteins were uniformly distributed throughout the axon and failed to become enriched at ankG$^+$ heminodes (heminodes Na$_v\beta4\Delta N^+ = 8.1 \pm 3.6\%$, $n = 138$, $N = 3$; heminodes Na$_v\beta4C28A^+ = 9.1 \pm 5.9\%$, $n = 42$, $N = 3$) (Fig. 7*B*,*C*). These results show that the recruitment of Na$_v\beta$4 to nodes of Ranvier, as with the AIS, depends on its direct interaction with Na^+ channel α subunits through a disulfide bond at C28.

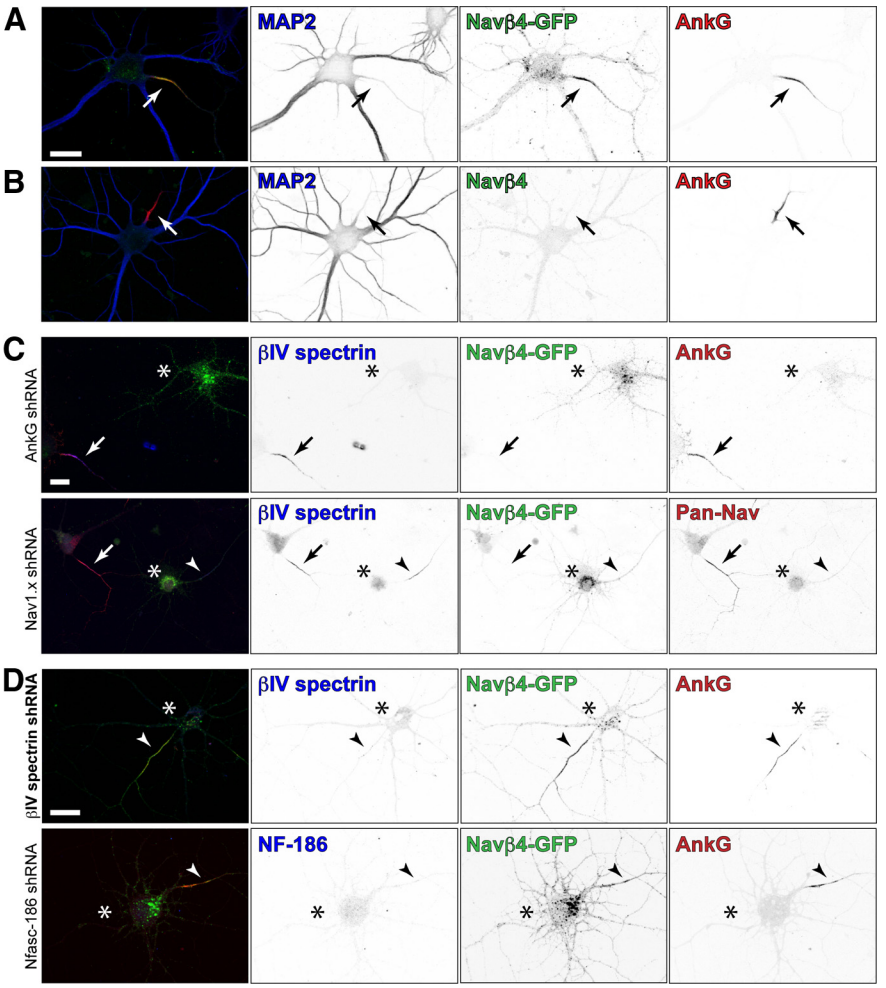

Figure 5. AnkG and Na$_v$1 α subunit expression are required for Na$_v\beta$4 AIS targeting. ***A***, Hippocampal neurons transfected with GFP-tagged Na$_v\beta$4 and immunostained for GFP (green), ankG (red), and MAP2 (blue). ***B***, Cultured hippocampal neurons immunolabeled for Na$_v\beta$4 (green), ankG (red), and MAP2 (blue). ***C***, ***D***, Immunostaining of cultured hippocampal neurons cotransfected with the indicated shRNA and FL Na$_v\beta$4–GFP constructs. Neurons were labeled with α-βIV spectrin or α-neurofascin-186 (blue), α-GFP (green), and α-ankG, or α-pan Na$_v$ channels (red). Transfected cells are marked with an *. Scale bars, 20 μm. ***C***, Immunostaining of cultured neurons transfected with shRNA targeting the AIS-organizing protein ankG or Na^+ channel α subunits, as indicated. Arrowhead indicates βIV spectrin$^+$/Na$_v\alpha^-$/Na$_v\beta4^-$ AIS in the bottom row, and arrows point toward neighboring control neuron AIS in all panels. ***D***, Knockdown of the AIS proteins βIV spectrin and neurofascin-186. Arrowheads highlight the location of Na$_v\beta4^+$ AIS in all panels.

Discussion

Open channel block by the C-terminal tail of Na$_v\beta$4 has been proposed as a potential mechanism for the generation of I_{NaR} in neurons (Grieco et al., 2005; Bant and Raman, 2010). Na^+ currents with resurgent kinetics have been suggested to stimulate neuronal excitability and promote repetitive firing (Khaliq et al., 2003). Extracellular recordings revealed that APs are first initiated in the AIS during both single-spike and bursting activity (Kole, 2011); hence, local regulation of Na^+ channel activity at the AIS is central to controlling neuronal firing properties. Here, we investigated the neuronal expression pattern and subcellular localization of Na$_v\beta$4. Our results link Na$_v\beta$4 expression and subcellular localization at the AIS and nodes of Ranvier to its proposed role in the generation of I_{NaR} and I_{NaP} and, consequently, to its contribution to repetitive spiking in neurons.

Patch-clamp experiments using focal application of TTX in perirhinal cortex suggest that I_{NaR} is primarily generated in the AIS (Castelli et al., 2007b). Notably, quantitative freeze-fracture immunogold studies of Na$_v$1.6, the Na^+ channel α subunit reported to carry the bulk of I_{NaR} in some cells (Raman et al., 1997; Khaliq et al., 2003; Grieco and Raman, 2004), suggest a 40-fold enrichment of Na$_v$1.6 at the AIS over the somatodendritic domain (Lorincz and Nusser, 2010). Thus, we reasoned that, if Na$_v\beta$4 is necessary for the generation of I_{NaR} in multiple cell types, then it should be strategically positioned to modulate the Na^+ channels involved in AP initiation, namely those enriched at the AIS. Using specific antibodies recognizing a unique epitope in the C-terminal tail of Na$_v\beta$4 (Fig. 1), we found cell-type-specific enrichment of Na$_v\beta$4 at the AIS of neuron classes known to express I_{NaR}, including cerebellar Purkinje neurons and subtha-

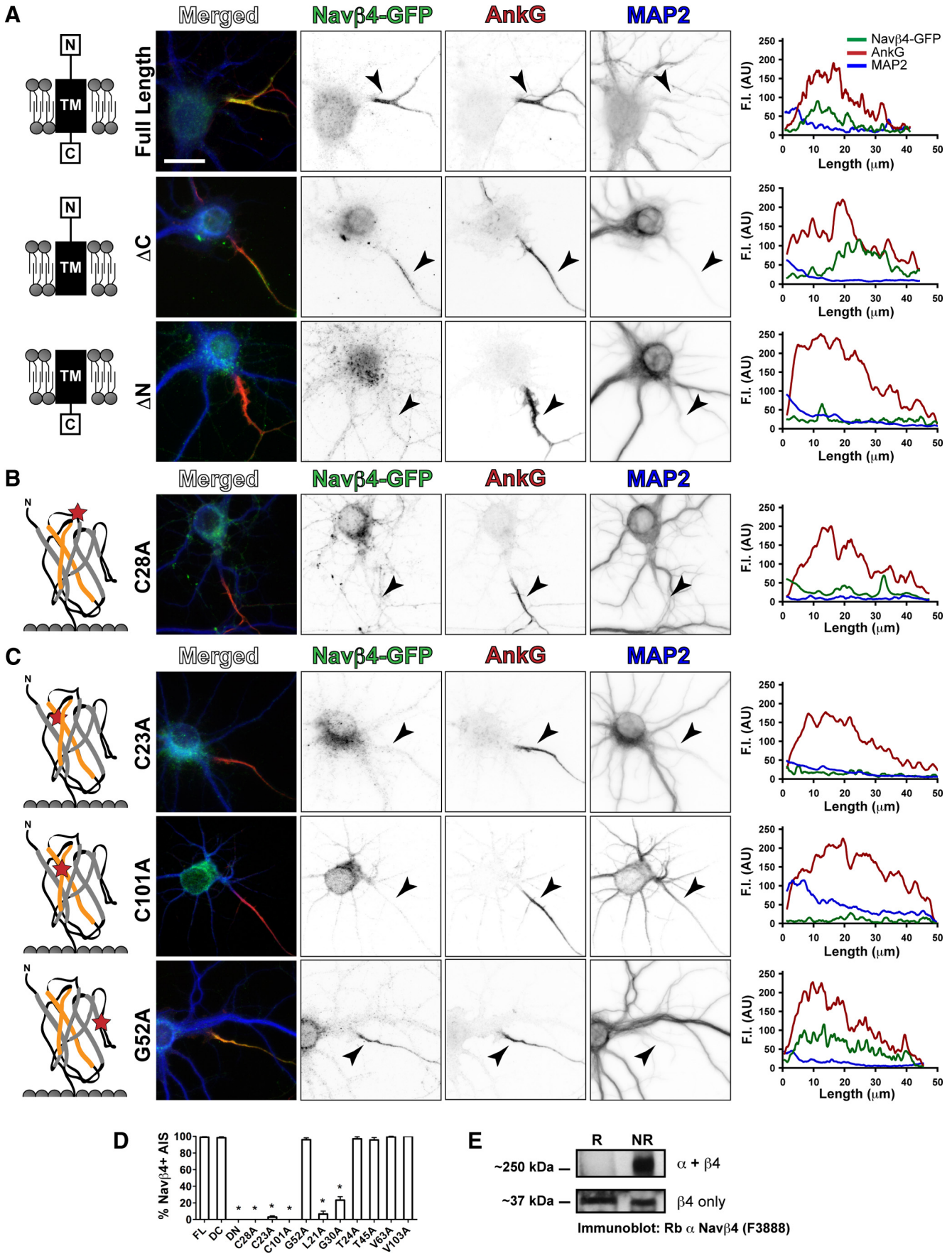

Figure 6. Cysteine 28 is required for $Na_v\beta4$ AIS localization. ***A***, Neurons transfected with FL, ΔC, or ΔN $Na_v\beta4$ constructs and immunostained for GFP (green), ankG (red), and MAP2 (blue). Longitudinal line scans through the AIS show fluorescence intensity (F.I.) of the $Na_v\beta4$–GFP (green), ankG (red), and MAP2 (blue) signals. ***B***–***E***, Immunostaining of (*Figure legend continues.*)

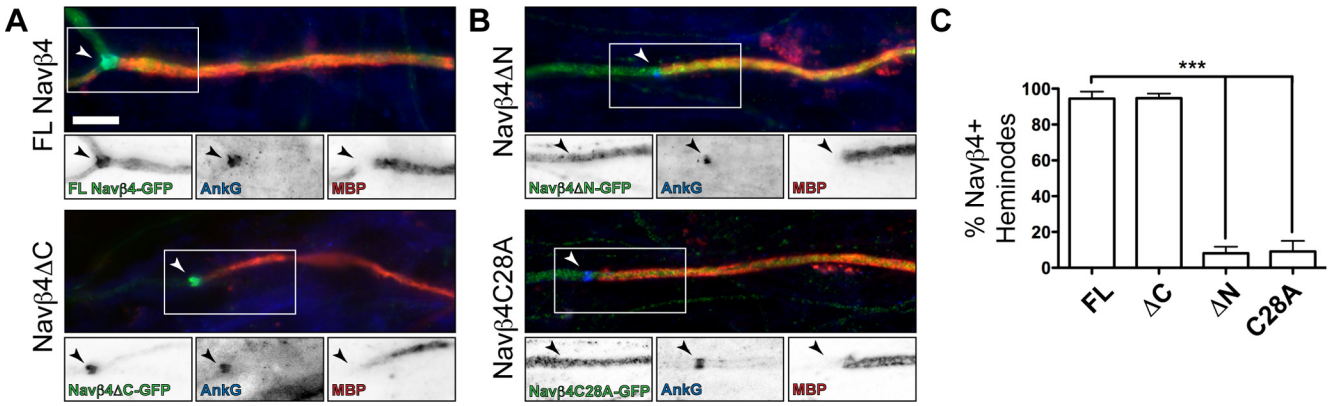

Figure 7. Cysteine 28 is required for $Na_v\beta4$ targeting to nodes of Ranvier. DRG neurons transfected with $Na_v\beta4$ expression constructs encoding FL-, ΔC- (***A***), ΔN-, and C28A–$Na_v\beta4$–GFP (***B***) constructs cocultured with myelinating Schwann cells. Myelinated axon segments were detected by immunostaining for MBP (red), whereas ankG immunoreactivity (blue) defined heminodes and forming nodes of Ranvier. The FL or mutant GFP-tagged $Na_v\beta4$ proteins were detected by GFP immunoreactivity (green). Scale bar, 10 μm. ***C***, Quantification of FL-, ΔC-, ΔN-, and C28A–$Na_v\beta4^+$ heminodes in the myelinating cocultures.

lamic neurons, among others (Fig. 2). Furthermore, we observed layer-specific enrichment of $Na_v\beta4$ at the AIS of cortical pyramidal neurons in layer V somatosensory cortex that was mostly absent from AIS in layers II/III, IV, and VI cortical pyramidal neurons. We also found $Na_v\beta4$ expression at the AIS of fast-spiking, PV^+ cortical interneurons and CB^+ brainstem interneurons (Fig. 3); however, $Na_v\beta4$ was also expressed in a subset of CB-expressing, PV^- neurons, suggesting that its expression is not restricted to high-frequency firing cell types. $Na_v\beta4$ protein expression in brainstem interneurons is consistent with recent single-cell transcript profiling results that found $Na_v\beta4$ expression to be a key marker differentiating fast-spiking inhibitory neurons from neighboring cells in the medial vestibular nucleus (Kodama et al., 2012). Finally, we observed strong $Na_v\beta4$ immunoreactivity in the TB, a site in which developmental increases in I_{NaR}, perhaps facilitated by $Na_v\beta4$ expression, contributes to rapid signal generation in these cells (Leão et al., 2006). Thus, $Na_v\beta4$ is enriched at the site of AP initiation (the AIS) of cell types characterized by high-frequency AP generation, some of which are known to carry I_{NaR}.

Similar to the AIS, Na^+ channels are densely clustered at nodes of Ranvier in myelinated axons for the efficient propagation of the AP. Here, we found that $Na_v\beta4$ is enriched at a subset of CNS and PNS nodes (Fig. 4). To our knowledge, I_{NaR} has not been directly recorded from nodes; however, non-inactivating channel kinetics underlying I_{NaP} have been measured at frog nodes of Ranvier (Dubois and Bergman, 1975), and some sensory neuron nodes in the DRG are capable of faithfully propagating AP trains approaching 1 kHz over long distances that can exceed 1 m (Wellnitz et al., 2010). We propose that the molecular mechanisms underlying fast spike generation at AIS are likely conserved at nodes. Intriguingly, a recent report on the contribution of nodes of Ranvier to repetitive firing revealed that nodal Na^+ channel activity critically contributes to burst probability in neocortical pyramidal neurons (Kole, 2011). This study showed that activity at the first node of Ranvier is essential for burst generation and that subthreshold I_{NaP} from distal axonal nodes of Ranvier contributes to the overall level of neuronal excitability. Whether or not I_{NaR} is expressed at nodes of Ranvier and the specific contribution of $Na_v\beta4$ to AP propagation at nodes remain active areas of investigation.

The contribution of $Na_v\beta4$ to repetitive firing may not be restricted to its role at the AIS nor even specifically in I_{NaR} but may also extend to facilitating I_{NaP} generation at nodes of Ranvier distributed throughout the entire length of the axon. Furthermore, it is possible that $Na_v\beta4$-modulated Na^+ channel gating at nodes of Ranvier may partially account for the molecular basis of subthreshold axonodal I_{NaP} generation. Facilitating I_{NaP} may be an additional mechanism by which $Na_v\beta4$ contributes to repetitive firing in neurons. Finally, resurgent current and $Na_v\beta4$ expression alone may not guarantee repetitive high-frequency firing. Instead, high-frequency firing likely depends not only on resurgent Na^+ current but also on the complement of high-threshold, rapidly deactivating K^+ currents found in specific neuron types.

By studying $Na_v\beta4$ trafficking to the AIS of cultured hippocampal pyramidal neurons that do not normally express $Na_v\beta4$, we were able to show that it can be recruited to the AIS without any special component found only in $Na_v\beta4$-expressing neurons. Specifically, our results show that $Na_v\beta4$ subunits are recruited to the AIS and nodes of Ranvier through a direct covalent disulfide bond with voltage-gated Na^+ channel α subunits, similar to $Na_v\beta2$ (Catterall, 1999; Yu et al., 2003). Although it remains unknown whether $Na_v\beta4$ binds to the α subunits before trafficking to these domains, our data suggest that any additional molecular interactions $Na_v\beta4$ may have with nodal or AIS cell adhesion molecules or ECM proteins are insufficient to either recruit or stabilize $Na_v\beta4$ at these sites. It will be interesting to determine which extracellular cysteine on the Na^+ channel α subunit is responsible for the interaction with $Na_v\beta4$. Although site-directed mutagenesis of FL Na^+ channels is technically quite difficult, it is possible and has been used to study Na^+ channel localization *in vivo* (Gasser et al., 2012). However, sequence alignment of brain Na^+ channels reveals 12 conserved extracellular cysteines, making it difficult to predict which of these forms the disulfide bond with $Na_v\beta4$. Furthermore, among the known variants of Na^+ channels, none affect an extracellular cysteine. Thus, determining where $Na_v\beta4$ interacts with the Na^+ channel

←

(*Figure legend continued.*) cultured hippocampal neurons transfected with $Na_v\beta4$-C28A (***B***) or the indicated $Na_v\beta4$ single point mutants (***C***) (C23A, C101A, and G52A). Neurons were immunolabeled using antibodies against GFP (green), ankG (red), and MAP2 (blue). Scale bar, 20 μm. ***D***, Quantitative analysis of $Na_v\beta4$ point mutant targeting to the AIS in cultured hippocampal neurons. ***E***, Western blotting for $Na_v\beta4$ in whole-brain membrane protein homogenates denatured in reducing (R) or non-reducing (NR) sample buffer. TM, Transmembrane.

α subunit will require future analyses of many Na^+ channel mutants.

$Na_v\beta4$ was discovered by mining expressed sequence tag databases for novel sequences with high homology to $Na_v\beta2$ (Yu et al., 2003). Examination of the human genome reveals that the family of Na^+ channel β subunit isoforms likely arose from a series of gene duplication events resulting in the four distinct transcripts. Given the heterogeneous expression pattern of $Na_v\beta4$, it will be interesting to uncover the mechanisms regulating transcriptional control of the various $Na_v\beta$ subunits. A limited phylogenetic analysis across 13 vertebrate species revealed conservation of key amino acid residues in the blocking peptide sequence of the C terminus of $Na_v\beta4$ (Lewis and Raman, 2011), suggesting that repetitive firing in Purkinje neurons, facilitated by $Na_v\beta4$-mediated resurgent kinetics, was selected for in vertebrates. Together, our data suggest that neuronal firing pattern diversity arises not only from variability in the expression of ion channel α subunits but also in cell-type-specific regulation of auxiliary protein expression. Furthermore, the specific subcellular localization of modulatory ion channel subunits, e.g., $Na_v\beta4$ targeting to AIS and nodes, likely determines the functional impact they have on neuronal computation (Nusser, 2009).

In summary, the data presented here identify $Na_v\beta4$ as a cell-type-specific component of the AIS and nodes of Ranvier and suggest a correlation between $Na_v\beta4$, resurgent Na^+ current, and repetitive firing. We also determined that $Na_v\beta4$ is recruited to these axonal electrogenic domains through direct interaction with the voltage-gated Na^+ channels enriched here. Our findings contribute to the idea that variability in the cell-type-specific expression pattern and subcellular distribution of ion channels and their modulatory subunits increases neuronal diversity, a key component underlying the evolution of higher cognition (Lorincz and Nusser, 2008; Nusser, 2009; Debanne et al., 2011).

References

Aman TK, Grieco-Calub TM, Chen C, Rusconi R, Slat EA, Isom LL, Raman IM (2009) Regulation of persistent Na current by interactions between beta subunits of voltage-gated Na channels. J Neurosci 29:2027–2042. CrossRef Medline

Bant JS, Raman IM (2010) Control of transient, resurgent, and persistent current by open-channel block by Na channel beta4 in cultured cerebellar granule neurons. Proc Natl Acad Sci U S A 107:12357–12362. CrossRef Medline

Barbieri R, Baroni D, Moran O (2012) Identification of an intra-molecular disulfide bond in the sodium channel $\beta1$-subunit. Biochem Biophys Res Commun 420:364–367. CrossRef Medline

Bean BP (2007) The action potential in mammalian central neurons. Nat Rev Neurosci 8:451–465. CrossRef Medline

Brackenbury WJ, Davis TH, Chen C, Slat EA, Detrow MJ, Dickendesher TL, Ranscht B, Isom LL (2008) Voltage-gated Na^+ channel beta1 subunit-mediated neurite outgrowth requires Fyn kinase and contributes to postnatal CNS development *in vivo*. J Neurosci 28:3246–3256. CrossRef Medline

Castelli L, Nigro MJ, Magistretti J (2007a) Analysis of resurgent sodium-current expression in rat parahippocampal cortices and hippocampal formation. Brain Res 1163:44–55. CrossRef Medline

Castelli L, Biella G, Toselli M, Magistretti J (2007b) Resurgent Na^+ current in pyramidal neurons of rat perirhinal cortex: axonal location of channels and contribution to depolarizing drive during repetitive firing. J Physiol 582:1179–1193. CrossRef Medline

Catterall WA (1999) Molecular properties of brain sodium channels: an important target for anticonvulsant drugs. Adv Neurol 79:441–456. Medline

Debanne D, Campanac E, Bialowas A, Carlier E, Alcaraz G (2011) Axon physiology. Physiol Rev 91:555–602. CrossRef Medline

Dubois JM, Bergman C (1975) Late sodium current in the node of Ranvier. Pflugers Arch 357:145–148. CrossRef Medline

Eshed Y, Feinberg K, Poliak S, Sabanay H, Sarig-Nadir O, Spiegel I, Bermingham JR Jr, Peles E (2005) Gliomedin mediates Schwann cell-axon interaction and the molecular assembly of the nodes of Ranvier. Neuron 47:215–229. CrossRef Medline

Feinberg K, Eshed-Eisenbach Y, Frechter S, Amor V, Salomon D, Sabanay H, Dupree JL, Grumet M, Brophy PJ, Shrager P, Peles E (2010) A glial signal consisting of gliomedin and NrCAM clusters axonal Na^+ channels during the formation of nodes of Ranvier. Neuron 65:490–502. CrossRef Medline

Galiano MR, Jha S, Ho TS, Zhang C, Ogawa Y, Chang KJ, Stankewich MC, Mohler PJ, Rasband MN (2012) A distal axonal cytoskeleton forms an intra-axonal boundary that controls axon initial segment assembly. Cell 149:1125–1139. CrossRef Medline

Garrido JJ, Giraud P, Carlier E, Fernandes F, Moussif A, Fache MP, Debanne D, Dargent B (2003) A targeting motif involved in sodium channel clustering at the axon initial segment. Science 300:2091–2094. CrossRef Medline

Gasser A, Ho TS, Cheng X, Chang KJ, Waxman SG, Rasband MN, Dib-Hajj SD (2012) An ankyrinG-binding motif is necessary and sufficient for targeting Nav1.6 sodium channels to axon initial segments and nodes of Ranvier. J Neurosci 32:7232–7243. CrossRef Medline

Grieco TM, Raman IM (2004) Production of resurgent current in Nav1.6-null Purkinje neurons by slowing sodium channel inactivation with β-pompilidotoxin. J Neurosci 24:35–42. CrossRef Medline

Grieco TM, Malhotra JD, Chen C, Isom LL, Raman IM (2005) Open-channel block by the cytoplasmic tail of sodium channel beta4 as a mechanism for resurgent sodium current. Neuron 45:233–244. CrossRef Medline

Hartwich K, Pollak T, Klausberger T (2009) Distinct firing patterns of identified basket and dendrite-targeting interneurons in the prefrontal cortex during hippocampal theat and local spindle oscillations. J Neurosci 29:9563–9574. CrossRef Medline

Hedstrom KL, Xu X, Ogawa Y, Frischknecht R, Seidenbecher CI, Shrager P, Rasband MN (2007) Neurofascin assembles a specialized extracellular matrix at the axon initial segment. J Cell Biol 178:875–886. CrossRef Medline

Hedstrom KL, Ogawa Y, Rasband MN (2008) AnkyrinG is required for maintenance of the axon initial segment and neuronal polarity. J Cell Biol 183:635–640. CrossRef Medline

Isom LL, De Jongh KS, Patton DE, Reber BF, Offord J, Charbonneau H, Walsh K, Goldin AL, Catterall WA (1992) Primary structure and functional expression of the beta 1 subunit of the rat brain sodium channel. Science 256:839–842. CrossRef Medline

Kaech S, Banker G (2006) Culturing hippocampal neurons. Nat Protoc 1:2406–2415. CrossRef Medline

Khaliq ZM, Raman IM (2006) Relative contributions of axonal and somatic Na channels to action potential initiation in cerebellar Purkinje neurons. J Neurosci 26:1935–1944. CrossRef Medline

Khaliq ZM, Gouwens NW, Raman IM (2003) The contribution of resurgent sodium current to high-frequency firing in Purkinje neurons: an experimental and modeling study. J Neurosci 23:4899–4912. Medline

Klausberger T (2009) GABAergic interneurons targeting dendrites of pyramidal cells in the CA1 area of the hippocampus. Eur J Neurosci 30:947–957. CrossRef Medline

Klausberger T, Somogyi P (2008) Neuronal diversity and temporal dynamics: the unity of hippocampal circuit operations. Science 321:53–57. CrossRef Medline

Kodama T, Guerrero S, Shin M, Moghadam S, Faulstich M, du Lac S (2012) Neuronal classification and marker gene identification via single-cell expression profiling of brainstem vestibular neurons subserving cerebellar learning. J Neurosci 32:7819–7831. CrossRef Medline

Kole MH (2011) First node of Ranvier facilitates high-frequency burst encoding. Neuron 71:671–682. CrossRef Medline

Kole MH, Stuart GJ (2008) Is action potential threshold lowest in the axon? Nat Neurosci 11:1253–1255. CrossRef Medline

Kole MH, Ilschner SU, Kampa BM, Williams SR, Ruben PC, Stuart GJ (2008) Action potential generation requires a high sodium channel density in the axon initial segment. Nat Neurosci 11:178–186. CrossRef Medline

Leão RN, Naves MM, Leão KE, Walmsley B (2006) Altered sodium currents in auditor neurons of congenitally deaf mice. Eur J Neurosci 24:1137–1146. CrossRef Medline

Lemaillet G, Walker B, Lambert S (2003) Identification of a conserved

ankyrin-binding motif in the family of sodium channel alpha subunits. J Biol Chem 278:27333–27339. CrossRef Medline

Lewis AH, Raman IM (2011) Cross-species conservation of open-channel block by Na channel beta4 peptides reveals structural features required for resurgent Na current. J Neurosci 31:11527–11536. CrossRef Medline

Lorincz A, Nusser Z (2008) Cell-type-dependent molecular composition of the axon initial segment. J Neurosci 28:14329–14340. CrossRef Medline

Lorincz A, Nusser Z (2010) Molecular identity of dendritic voltage-gated sodium channels. Science 328:906–909. CrossRef Medline

McEwen DP, Isom LL (2004) Heterophilic interactions of sodum channel beta1 subunits with axonal and glial cell adhesion molecules. J Biol Chem 279:52744–52752. CrossRef Medline

Nusser Z (2009) Variability in the subcellular distribution of ion channels increases neuronal diversity. Trends Neurosci 32:267–274. CrossRef Medline

Palmer LM, Stuart GJ (2006) Site of action potential initiation in layer 5 pyramidal neurons. J Neurosci 26:1854–1863. CrossRef Medline

Pan F, Beam KG (1999) The absence of resurgent sodium current in mouse spinal neurons. Brain Res 849:162–168. CrossRef Medline

Raman IM, Sprunger LK, Meisler MH, Bean BP (1997) Altered subthreshold sodium currents and disrupted firing patterns in Purkinje neurons of Scn8a mutant mice. Neuron 19:881–891. CrossRef Medline

Raman IM, Bean BP (2001) Inactivation and recovery of sodium currents in cerebellar Purkinje neurons: evidence for two mechanisms. Biophys J 80:729–737. CrossRef Medline

Rasband MN, Kagawa T, Park EW, Ikenaka K, Trimmer JS (2003) Dysregulation of axonal sodium channel isoforms after adult-onset chronic demyelination. J Neurosci Res 73:465–470. CrossRef Medline

Rhodes KJ, Keilbaugh SA, Barrezueta NX, Lopez KL, Trimmer JS (1995) Association and colocalization of K^+ channel α- and β-subunit polypeptides in rat brain. J Neurosci 15:5360–5371. Medline

Susuki K, Raphael AR, Ogawa Y, Stankewich MC, Peles E, Talbot WS, Rasband MN (2011) Schwann cell spectrins modulate peripheral nerve myelination. Proc Natl Acad Sci U S A 108:8009–8014. CrossRef Medline

Wellnitz SA, Lesniak DR, Gerling GJ, Lumpkin EA (2010) The regularity of sustained firing reveals two populations of slowly adapting touch receptors in mouse hair skin. J Neurophysiol 103:3378–3388. CrossRef Medline

Yang Y, Lacas-Gervais S, Morest DK, Solimena M, Rasband MN (2004) βIV spectrins are essential for membrane stability and the molecular organization of nodes of Ranvier. J Neurosci 24:7230–7240. CrossRef Medline

Yang Y, Ogawa Y, Hedstrom KL, Rasband MN (2007) betaIV spectrin is recruited to axon initial segments and nodes of Ranvier by ankyrinG. J Cell Biol 176:509–519. CrossRef Medline

Yu FH, Westenbroek RE, Silos-Santiago I, McCormick KA, Lawson D, Ge P, Ferriera H, Lilly J, DiStefano PS, Catterall WA, Scheuer T, Curtis R (2003) Sodium channel $\beta4$, a new disulfide-linked auxiliary subunit with similarity to beta2. J Neurosci 23:7577–7585. Medline

Zhang X, Davis JQ, Carpenter S, Bennett V (1998) Structural requirements for association of neurofascin with ankyrin. J Biol Chem 273:30785–30794. CrossRef Medline

Zhang Y, Bekku Y, Dzhashiashvili Y, Armenti S, Meng X, Sasaki Y, Milbrandt J, Salzer JL (2012) Assembly and maintenance of nodes of Ranvier rely on distinct sources of proteins and targeting mechanisms. Neuron 73:92–107. CrossRef Medline